INL/JOU-21-65504-Revision-0

Separation of cobalt, nickel, and manganese in leach solutions of waste lithium-ion batteries using Dowex M4195 ion exchange resin

December 2021

Tedd E Lister, Mark Strauss, Luis A Diaz Aldana, Joshua S McNally, John R Klaehn

INL/JOU-21-65504-Revision-0

Separation of cobalt, nickel, and manganese in leach solutions of waste lithium-ion batteries using Dowex M4195 ion exchange resin

Tedd E Lister, Mark Strauss, Luis A Diaz Aldana, Joshua S McNally, John R Klaehn

December 2021

Idaho National Laboratory
Idaho Falls, Idaho 83415

http://www.inl.gov

Prepared for the
U.S. Department of Energy
Under DOE Idaho Operations Office
Contract DE-AC07-05ID14517

Separation of Cobalt, Nickel, and Manganese in Leach Solutions of Waste Lithium-Ion Batteries Using Dowex M4195 Ion Exchange Resin

M. L. Strauss, L. A. Diaz, J. McNally, J. Klaehn, and T. E. Lister
Idaho National Laboratory
2525 Fremont Avenue, Idaho Falls, Idaho, USA 83402
*(*Corresponding author: Tedd.Lister@inl.gov, 208-526-4320)*

Abstract

Current methods to separate and recover critical metals from waste lithium-ion battery (LIB) scrap require multiple unit operations that involve selective leaching and a combination of separation methods. These methods include impurity removal, solvent extraction, ion exchange, and precipitation, to achieve high purity Co and Ni products. In this paper an efficient extraction strategy was developed to individually separate Ni and Co from a LIB leachate that was generated from an electrochemical leaching process. By using Dowex M4195 resin, as the only method of separation, additional impurity removal operations were not needed. After loading and eluting, three different fractions were obtained: 99.0% Ni concentrate, 98.5% Co concentrate, and a Li/Mn rich concentrate allowing the separation of Ni, Co and Mn. The developed process is then presented as an alternative for metal recovery from leachates from scrap LIBs with minimum chemical addition and pH adjustment.

Keywords

Critical materials, Lithium-ion batteries, Recycling, Cobalt, Ion exchange

1. Introduction

The current trend to substitute internal combustion engine vehicles with an electrified alternative is forecasted to increase at a compound annual grow rate of 13% (Grand View Reasearch, 2020). It is expected that 1.2 million tons of end-of-life (EOL) lithium ion batteries (LIBs), will be available by 2030, a six-fold increase from 2018 (Nguyen et al., 2021; Willuhn, 2019). Although some EOL LIBs could be repurposed for stationary energy storage, between 0.4 to 1 million tons of generated LIB scrap could be available for recycling (DeRousseau et al., 2017). Since 2019, approximately two dozen international battery recycling companies have been operating at the commercial or pilot scale (Pinegar and Smith, 2019). However, current process capacity does not exceed 100,000 tons of EOL LIB per year, and the current recycling rate is only about 5% in North America (Jacoby, 2019; Linnenkoper, 2019). Recycling metals from EOL LIB is not only essential to waste minimization and environmental stewardship, but also a source of critical materials, which can contribute towards supply chain stabilization.

One of the major challenges associated with metal recycling from LIB scrap is the continuously evolving chemistry of LIB cathodes. While Co has remained as a key element in LIB cathodes because it provides good conductivity and high stability throughout the LIB's cycle life (Manthiram, 2020; Mizushima et al., 1981). The Co supply chain has several challenges associated with low abundance and geographical concentration (Campbell, 2019; Olivetti et al., 2017). As a result, the price uncertainty of Co is a limitation in expanding future battery manufacturing, whereas efforts to decrease or eliminate the use of Co in LIBs cathodes by substitution with less expensive and more abundant metals, such as Ni, Mn, and Al (Armand et al., 2020; Lee et al., 2001; Manthiram, 2020; Zeng et al., 2019), could affect the interest on battery recycling from an economic prospective. Therefore, viable alternatives to recover value and critical metals from EOL LIBs require novel and robust chemical processing techniques that can accommodate changing metal compositions.

At least three strategies can be considered for the recycling of EOL LIB. Non-destructive approaches such as direct recycling minimize chemical processing while preserving the value present in battery materials, a cathode-to-cathode approach (Larouche et al., 2020; Sloop et al., 2019). Pyrometallurgical processing of LIBs, can accept all battery types without significant pre-processing or physical separation. However, it is destructive to graphite, electrolyte and plastic recovery, has higher direct energy requirements, produces toxic off-gases, and has low recoveries of Li and Mn (Pinegar and Smith, 2019). Alternatively, hydrometallurgical processes can achieve a more comprehensive recovery of all the valued elements in LIBs with high selectivity and efficiency at the expense of significant chemical consumption, which is finally reflected in high cost and environmental impacts (Xu et al., 2020).

Due to the high concentration of Ni and Co in LIBs, Co/Ni separation technologies that evolved from Ni laterite hydrometallurgy have influenced the unit operations for LIB recycling. Current methods for the separation of LIB's metals include selective leaching, solvent extraction (SX), and selective precipitation. Complexing reagents first developed for use in Ni laterite mines have been demonstrated to efficiently separate metals from LIB leachates (Atia et al., 2019; Chiu and Chen, 2017; Kurşunoglu, 2019). Although SX may be amenable to high throughput industrial operations, the definition of a flowsheet is highly dependent on factors such as, leachate pH, metal concentration, and the presence of impurity metals such as Fe, Al, and Cu. Impurity metal removal is an essential operation, as co-extraction, strong bonding, and even solvent degradation can affect downstream refinement processes (Ocio and Elizalde, 2011; Pranolo et al., 2010). Alternatives for metal impurity removal include the use of target reagents, such as Di-2-ethylheyxl phosphoric acid (D2EHPA), Acorga 5640, and Ionquest 801 (Agarwal et al., 2019; Nayl et al., 2015; Pranolo et al., 2010), or the use of selective precipitation by pH adjustment (Peng et al., 2019). In both cases the intensive use of chemicals and poor selectivity affect the recovery efficiencies for valuable metals along with the economic performance of the process (Virolainen et al., 2021).

Ion exchange (IX) is an alternative to SX that uses little to no volatile organic solvents, needs limited impurity metal removal before separation, is operational over a wide pH range, has better selectivity in some multi-metal systems, and can potentially decrease operational and capital costs (Mendes and Martins, 2004). While it has been used to separate metals in mining and alkaline battery recycling operations, it is just gaining traction in the processing LIB leachates (Lannoo et al., 2019; Virolainen et al., 2021). Dowex M4195 (Dowex), a bispicolylamine ion exchange resin, has been used industrially to remove Ni from Co electrolyte at the Vale Port Colborne Ni Refinery (Sole et al., 2017). Similarly, it is employed at the Chambishi Metals refinery in Zambia to recover Ni (Rosato et al., 1984; Swartz et al., 2009). Several papers have also demonstrated its high selectivity for Ni and Co separation at a wide pH range including lower pH between 1-2 (Chiu and Chen, 2017; Grinstead, 1984; Liebenberg et al., 2013). The possibility to operate at lower pH ranges is fundamental to process battery leachates as this leads to decreased chemical consumption as pH adjustment is unnecessary (Mendes and Martins, 2004).

At pH=4, the Dowex resin is selective in the following order: Cu>>Ni>Fe(III)>Zn>Co>Cd>Fe(II) (Grinstead, 1984; Mendes and Martins, 2004; Nagib et al., 1999; Pranolo et al., 2010). Dowex has a strong affinity for Cu and requires the use of strong acids (500 g/L H_2SO_4) or concentrated ammonia for elution. Presence of Cu in the leachates reduces the cyclability of the Dowex column thereby decreasing its performance over time. This has been identified as one the main disadvantages for the processing of Cu containing leachates, such as those obtained from the leaching of LIBs (Sole et al., 2017). Alternatives, such as pre-processing for impurity removal, or the use of a pre-IX process to remove Cu were implemented (Sole et al., 2018, Harris & White, 2019). Similarly, D2EHPA has been tested as a pre-treatment to remove Fe and Al from leachates of spent ammonia cracker catalysts before Dowex separation (Sadanandam et al., 2008). The low affinity of Dowex towards Mn adsorption has shown to be useful in the purification of Mn leachates used towards the production of MnO_2 (Diniz et al., 2005).

In a previous work, we reported the development of an electrochemically assisted leaching (EC-leaching) process for the extraction of metals from LIB black mass. In the EC-leaching process Fe(II), in small concentrations (ca. 10 mM) in H_2SO_4, is used to reduce and extract Co, Mn, Ni, and Li from LIB's black mass (Diaz et al., 2020). Fe(III) produced from the leaching process is reduced to Fe(II) at the cathode of an electrochemical cell and new Fe(II) is generated to continue with the extraction cycle until completion. At the potentials in which Fe(III) is reduced to Fe(II), Cu(II) is also reduced to Cu metal and deposited on the cathode, thus removing Cu from the leachate solution. The electrochemical cell configuration reduces acid consumption, operates at high pulp densities, and facilitate control the final pH of the leachate. Also, the EC-leaching process makes it possible to obtain LIB leachates with a final pH between 1 to 3 without chemical addition to adjust (increase) pH. Considering the advantages provided by the electrochemically produced leachate in terms of pH, removal of Cu, and the limited amount of Fe in the leachate, where Fe is in the reduced form Fe(II), this work developed a flowsheet to obtain high purity Co and Ni products, using only Dowex M4195 without the need to use additional metal impurity removal from a LIB leachate obtained through the EC-leaching process.

2. Materials and Methods

2.1 Materials

All the chemicals used: H_2SO_4 (Fisher Chemical), $FeSO_4$ (Sigma Aldrich), NH_4OH. (Fisher Scientific), and ammonium acetate 99% ($NH_4(CH_3CO_2)$ MP Biomaterials), were ACS certified, and solutions were prepared with deionized (DI) water (18MΩ). Dowex M4195 (or Ambersep M4195) resin was obtained through Sigma Aldrich. LIB black mass was provided by Retriev Technologies and has an elemental composition reported elsewhere (Diaz et al., 2020). The LIB leachate solution was obtained through an EC-leaching method previously described (Diaz et al., 2020). 24 g of LIB black mass, along with 180 mL 1 M H_2SO_4 with 10 mM $FeSO_4$ were processed at the cathode compartment of an electrochemical cell achieving >99% metals dissolution. A pH pump with 2 M H_2SO_4 was used to adjust the final pH to pH~1. A typical concentration of the feed leachate is shown in Table 1 (Feed CA).

2.2 Breakthrough curves and process development

Dowex resin was packed into clear PVC columns, 80 mm long, 20 mm in diameter, and the bed volume (BV) was 20 mL. After packing, a wetting procedure was followed to prevent pressure buildup in the column due to expansion of the resin. Two peristaltic pumps (Cole Parmer MasterFlex C/L Pump) were used to feed solutions to the column at a rate of 0.25 mL/min.

The proposed separation strategy consists in a series of columns where Ni is first removed from the leachate in the first set of columns followed by the removal of Co in a second set of columns after pH adjustment (Fig. 1). For the breakthrough analysis, the LIB leachate solution, without any pH adjustment, was fed from the bottom of a single Column A (CA) to study Ni separation. After 80 mL of effluent from CA was collected, $NH_4(CH_3CO_2)$ was added to reach a concentration of 0.5 M, followed by NH_4OH hydroxide 30-35% addition dropwise to adjust the pH above 4.0. This pH adjusted solution was used as the feed for Co separation through a single Column B (CB). Backflow (top to bottom) was used for column washing and elution.

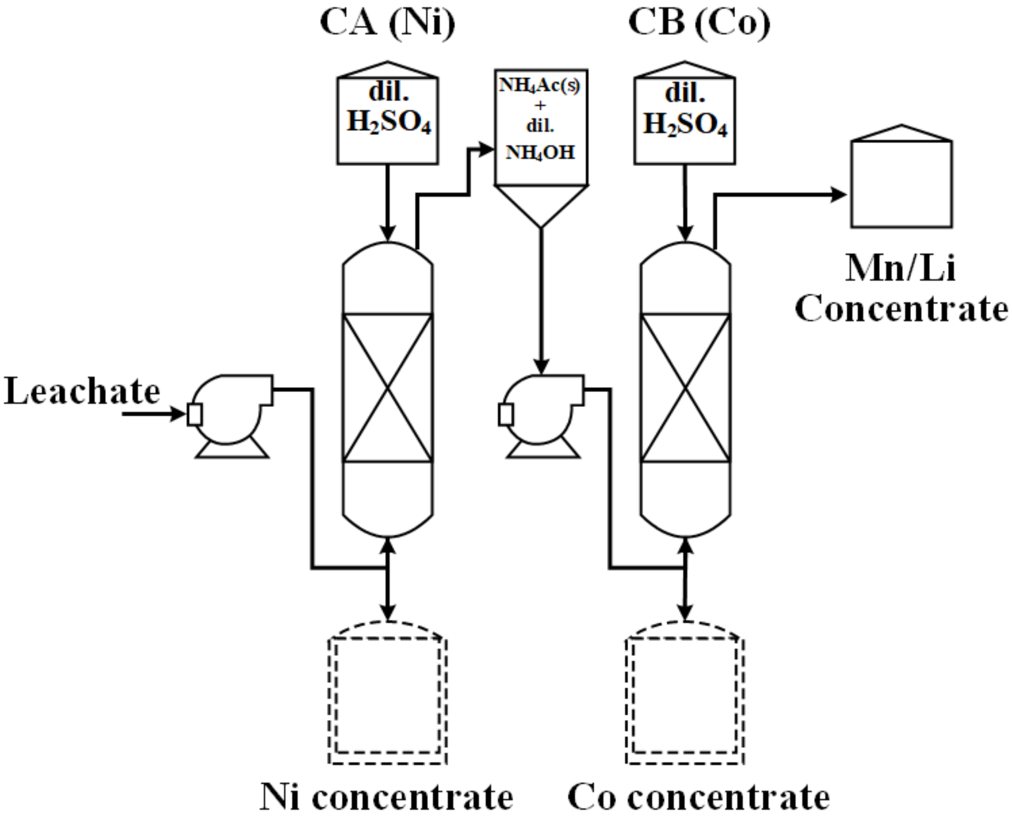

Fig. 1. Process flow diagram for Ni concentrate, Co concentrate, Mn/Li concentrate beginning with leachate

To further improve metal separation and purity experiments were performed using sets of two columns for each separation, respectively. Information from the breakthrough tests was used to determine the loading and eluting strategies for Ni and Co sets, respectively.

2.3 Analysis

Elemental analysis of the metals in the leachate and produced solutions were performed using an Agilent Technologies 240 FS Atomic Absorption Spectrometer (AAS) Q. Calibration was performed using commercially prepared standards (VGH and Spex). X-ray diffraction (XRD) spectroscopy was performed using a Bruker D8 Advance diffractometer operated at 40 kV and 40 mA, with a copper (Cu) target (K = 1.54060 Å). Materials phase and characterization were done using the software EVA and a 2010 ICDD data base (Gates-Rector and Blanton, 2019).

3. **Results and Discussion**

The development of an IX process for metals recovery requires an understanding of separation factors given specific feed conditions, e.g., pH, concentration, impurity quantities, etc. The method employed in this study utilized two columns to achieve Ni and Co separation and recovery from LIB leachate, without significant modification of the feed solution. The breakthrough profiles of the extracted metals were analyzed, and the data was used to initiate the development of a process that optimizes the recovery of Ni and Co.

3.1 Breakthrough curves

The purpose of employing two sets of columns in series was to create three discrete downstream products: a Ni concentrate, a Co concentrate, and Mn/Li concentrate. Although the adsorption capacity for both Co and Ni decrease in relationship to pH, the ratio of Ni/Co adsorption constants increase by a factor of 148% with a pH decrease from 2 to 1.5 (Rosato et al., 1984). By feeding the leachate directly after extraction at a pH 1-2, CA is selectively loaded with Ni over Co. The breakthrough curves shown in Fig. 2 clearly demonstrates that Ni is selectively adsorbed, while Co and the other elements present in the LIB leachate pass through the column without significant interactions achieving saturation within 0.75 BVs vs. 4 BVs for Ni.

Table 1. Concentration of feed solutions for CA and CB, and final concentration of the obtained Li/Mn concentrate

	pH	Co (g/L)	Ni (g/L)	Mn (g/L)	Li (g/L)	Al (g/L)	Fe (g/L)	Zn (g/L)	Cu (g/L)
Feed CA	1.10	19.00	7.00	5.00	3.00	0.60	0.40	0.05	0.00
Feed CB	4.19	13.00	0.90	3.00	2.00	0.20	0.30	0.03	0.00
Li/Mn Concentrate	3.05	0.06	0.06	3.00	2.00	0.20	0.03	0.00	0.00

Aluminum was not measured for the breakthrough experiments because it was reported to have no interactions with Dowex M4195 (Liebenberg et al., 2013). The pH profile of the effluent is shown in the inset of Fig. 2. The first collected samples have a pH higher than the feed solution, which can be explained by the displacement of water retained within the packed column and agrees with the metal concentration profiles. Following this, the pH decreases as adsorbed Ni displaces a hydrogen proton (H^+) from the original protonated resin (Grinstead, 1984). As fewer metal ions get adsorbed, fewer H^+ ions are released until the pH of the effluent reaches the pH of the feed at saturation. A total of 267 mg of Ni (31% of the fed Ni) were estimated to be adsorbed to the column.

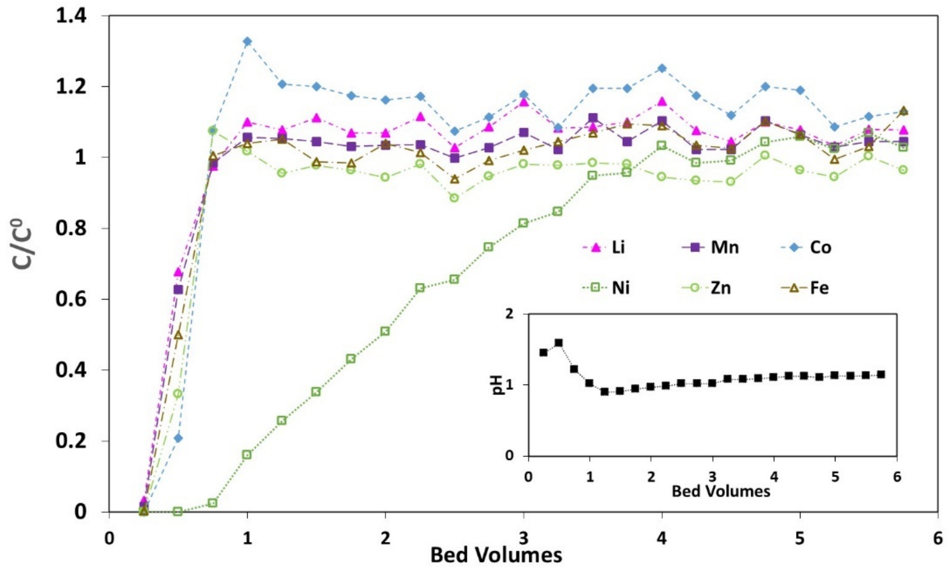

Fig. 2. Load profile for CA for the effluent collected for a starting feed of pH=1.1. The inset graph shows the corresponding pH profile.

Effluent fractions from which up to 80% of the Ni was removed were collected from several experiments. The mixed collection of effluents from CA were adjusted to pH 4-4.2 using $NH_4(CH_3CO_2)$ and 30-35%

NH_4OH. $NH_4(CH_3CO_2)$ acts as buffer and should not affect the solubility of metals at higher pH. While ammonium and acetate can weakly coordinate with transition metals, the performance of chelating resins like Dowex have shown to be unimpaired by weak complexing ions in solution (Koivula et al., 2000; Mendes and Martins, 2004). The pH adjusted effluent from CA was fed to CB to remove the Co and obtain a Mn/Li effluent. Fig. 3 shows the breakthrough curves of metals in CB. A total of 578 mg of Co (52% of the fed Co) were estimated to be adsorbed to the column. Higher adsorption capacities can be achieved at higher pH, and therefore, more Co (in comparison with Ni in CA) could be adsorbed.

Mn shows little to no affinity to Dowex even at the higher pH as reported by Diniz et al. (2005) and Grinstead (1984). A similar conclusion can be drawn for Li whose profile closely follows that of Mn. Fe, Zn, Co and Ni are initially adsorbed on CB without any significant difference. However, after 0.75 BVs, Fe begins to be released possibly due to displacement by other metals with higher affinity. These results agree with the Dowex affinity reported previously and demonstrates one of the benefits to integrate the EC-leaching process with IX separation (Grinstead, 1984; Mendes and Martins, 2004; Nagib et al., 1999; Pranolo et al., 2010). Since Fe is mostly present as Fe(II), it can be displaced by Co in CB. A different scenario is observed for Zn, which shows a higher adsorption affinity than Co, in agreement with the reported affinity series. However, Zn's original concentration in the feed solution is three orders of magnitude lower than that of Co (Table 1). In addition, Fig. 3 shows that the depleted Ni feed never reached breakthrough. The pH profile in CB follows the trend observed with CA where a significant pH decrease is caused by ion exchange.

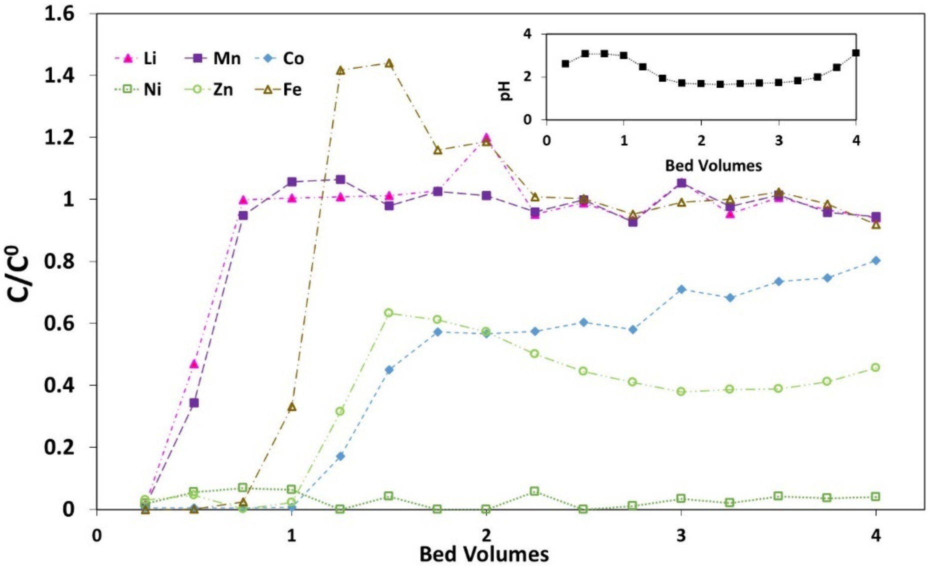

Fig. 3. Load profile for the effluent collected from CB. The inset graph shows the corresponding pH profile.

3.2 CA and CB Elution

After CA and CB were loaded with Ni and Co, respectively, the columns were thoroughly washed from top to bottom with more than 10 BV of DI water individually to remove unbound metal ions. Elution of metals adsorbed in CA was performed with 55 mL 2 M H_2SO_4. Elution profiles on Fig. 4 show that Ni was the main element adsorbed in CA. The average Ni purity of the eluted fraction is 97.9%, with a maximum of 99.9% observed at 1.5 BV. Elution profiles also show Co as the main contaminant in the Ni concentrated stream. The total amount of Ni recovered in the elution corresponds to 87.9% of the total adsorbed Ni.

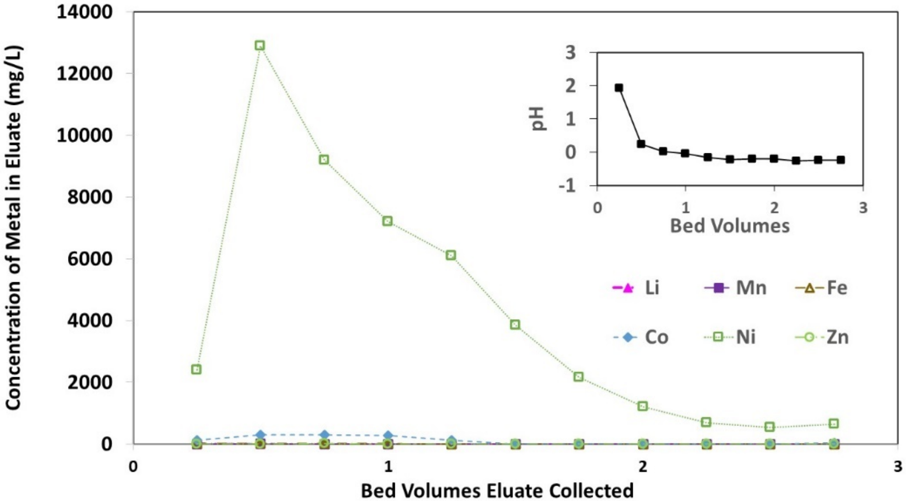

Fig. 4. Elution profile for Ni concentrate eluted from CA. The inset graph shows the corresponding pH profile.

Loaded CB was eluted with 55 mL 1 M H_2SO_4. Elution profiles in Fig. 5 show that Co was the main element adsorbed in CB. The average Co purity of the eluted fraction is 95.8%, with a maximum of 98.8% observed at 0.50 BV. Ni, the most abundant impurity in the Co concentrate, appeared only after the pH of the eluted solution dropped below pH 2. Rosato et al. (1984) demonstrated the possibility to achieve split elution of Co and Ni by controlling the concentration of the elution acids. Therefore, this technique, could be used not only to achieve higher Co purities from the elution of CB, but also to remove the minor Co contaminants observed during the elution of CA. Only 59% of the adsorbed Co was recovered in the eluate. Significant Co quantities were lost to the wash which suggests relatively weak Co adsorption.

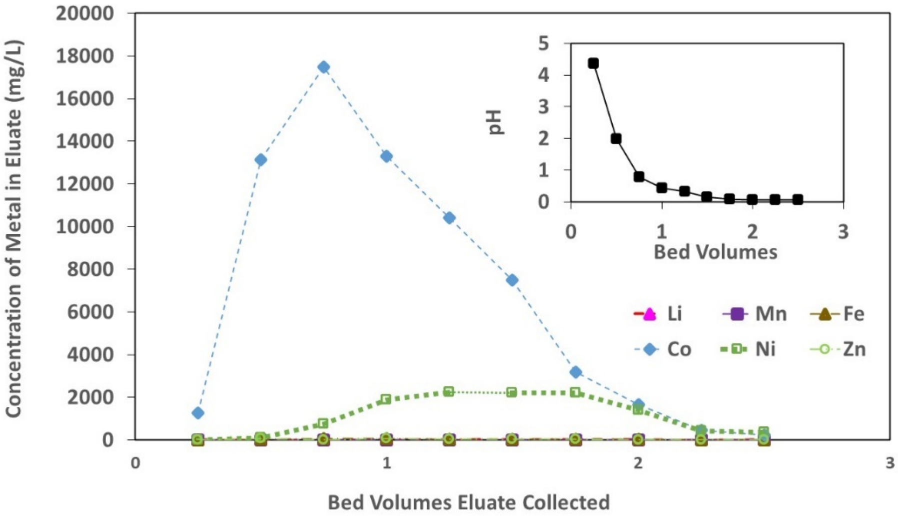

Fig. 5. Elution profile for Co concentrate eluted from CB. The inset graph shows the corresponding pH profile.

4. **Improved Methods**

4.1 **Ni column set loading and elution.**

Most industrial IX operations employ two or more columns to achieve equilibration of the lead column (1st column) while maintaining the mass transfer zone within the adsorption region. Therefore, a second packed column, in series with the lead column was added to each column set, Co and Ni, respectively. While breakthrough experiments provided important information about the adsorption capacity of Dowex resin to process LIB leachates, this improved method demonstrated high recovery and purity of the metals of interest, as well as minimization of waste generation by reducing the volume of solution required for washing and elution.

The total volume of solution fed to the CPA was calculated from the estimated amount of Ni adsorbed during the breakthrough experiments (267 mg ±10%). Fig. 6 shows loading, washing, and elution for CPA for one cycle. In a following cycle the second column in the series takes the place of the lead column and the same operation is repeated.

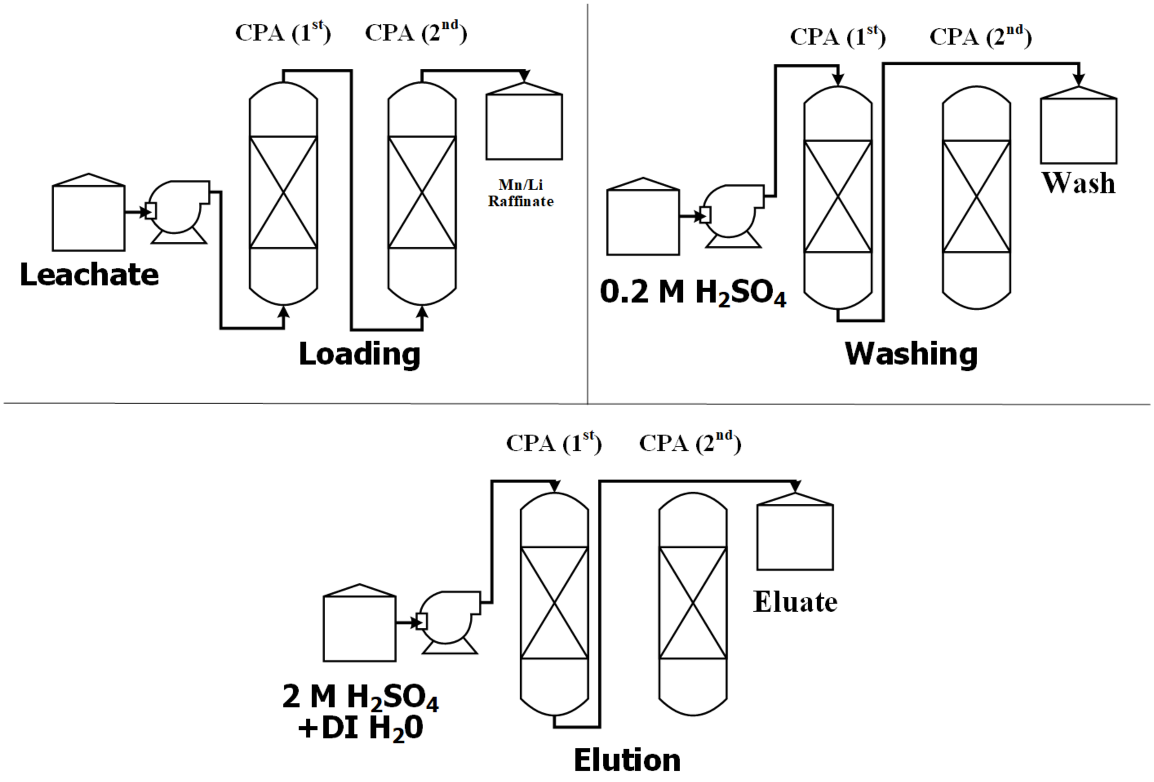

Fig. 6. Operation sequence for loading, washing and elution of CPA

Fig. 7 shows the metals concentration profile in the effluent of CPA. It is clearly observed that Ni is preferentially adsorbed over the other metals in solution. In Table 2, the mass balance of metals through the CPA confirms that the interaction of all metals with the resin, besides Ni, is minimal. Moreover, it was confirmed that Al is not adsorbed and leaving with the effluent. The advantage of extending the mass transfer zone to a second column can be observed by the fact that Ni reached a 0.2 effluent/feed concentration ratio (C/C^0) at twice as many BV as observed in the breakthrough of a single column (Fig.

2). In addition, the pH of the effluent is lower than the feed indicating that ion exchange is continuing.

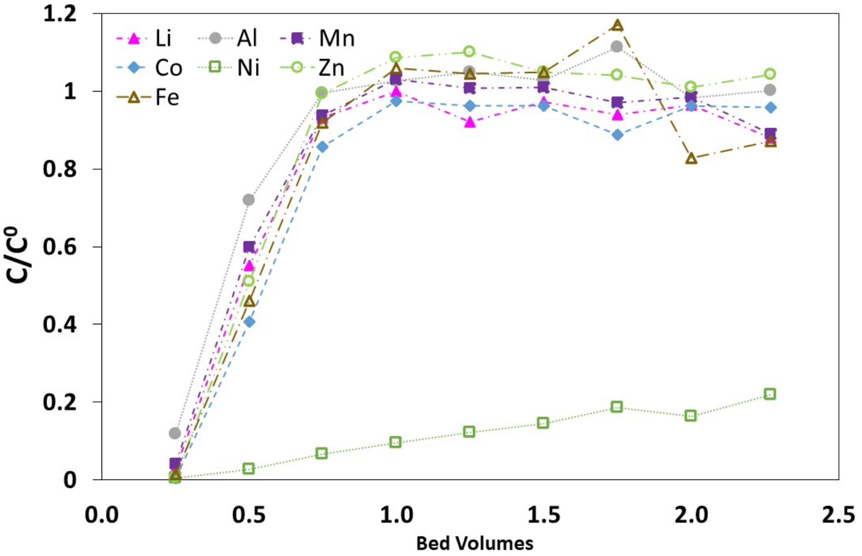

Fig. 7. Load profile for the effluent collected after the feed solution is passed through CPA. The inset graph shows the corresponding pH profile.

After loading, the lead column to CPA was washed with 40 mL of 0.2 M H_2SO_4 to remove possible traces of Co still present in the column, following the split elution concept (Rosato et al., 1984). The leftmost section of Fig. 7 shows that Co, but also significant amounts of Ni, were washed out of the column. 34.1% Ni was removed with the wash as reported in Table 2. A more diluted acid could be utilized for washing. Nevertheless, Ni and Co in the wash solution should not be considered as lost because the wash solution can be re-used to produce leaching solutions in a closed loop process. Ni was eluted with 10 mL of 2 M H_2SO_4 followed by 20 mL of DI water. 36.2% of the loaded Ni reports to the eluate, and the average Ni purity of the eluted fraction was 99.7 %.

16.7% of the Ni was unaccounted for in neither the effluent, wash, nor eluate. The low Ni concentration and pH of the last elution point on Fig 7. suggest that unrecovered Ni should have been adsorbed to the second column in the CPA series. In the following cycle column 2 takes as the lead column allowing for the adsorbed Ni to be recovered. Table S1 (supporting file) shows that complete Ni accountability can be achieved after performing complete cycles of loading and elution.

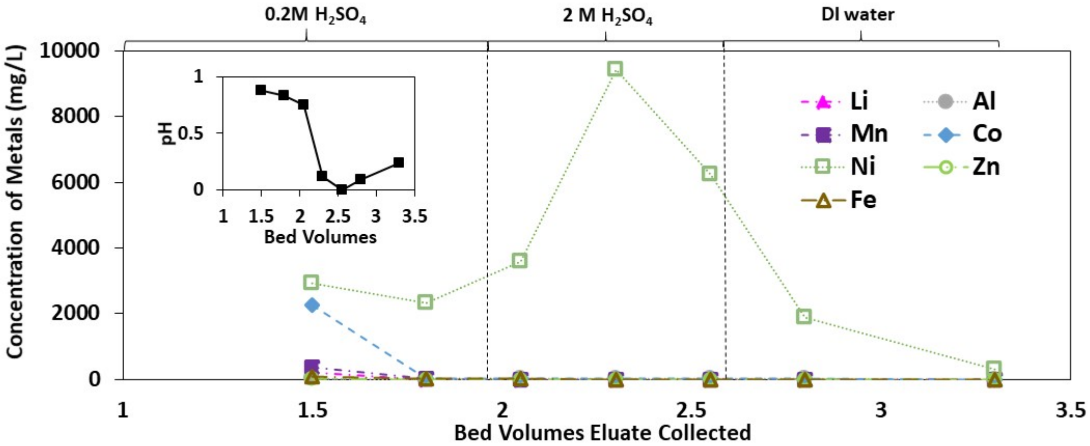

Fig. 8. Profile for Ni concentrate eluted from CPA. The inset graph shows the corresponding information for the pH.

Table 2. Mass balance of metals through processing through CPA is shown. The feed solution pH was 1.1, and the volume was 40 mL.

	Li	**Al**	**Mn**	**Fe**	**Co**	**Ni**	**Zn**
Feed (ppm)	3376.38	413.46	5440.04	681.51	21506.39	7491.23	50.83
% Effluent	90.77	101.43	94.27	93.64	88.17	13.05	99.03
% Wash	4.64	4.17	5.26	8.77	7.89	34.05	7.72
% Eluate	0.01	0.54	0.01	0.09	0.02	36.23	0.69
% Not Eluted	4.58	0.00	0.47	0.00	3.93	16.68	0.00
% Total	100.00	106.15	100.00	102.50	100.00	100.00	107.44

4.2 **Co column set loading and elution**

Due to the weak adsorption of Co with Dowex, the purpose of the second column in CPB goes beyond extending the mass transfer zone, but also to serve as Co trap during washing. Loading, washing and elution for CPB is shown in Fig. 9.

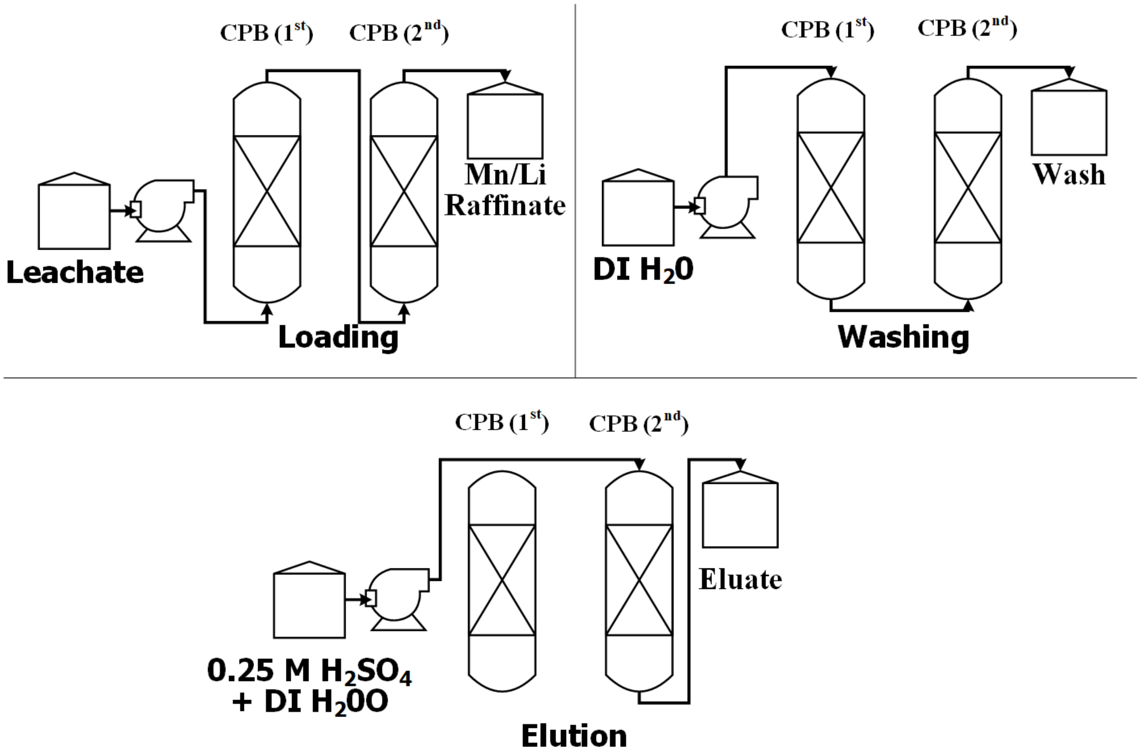

Fig. 9. Operation sequence for loading, washing and elution of CPB.

The total volume of pH adjusted solution (pH=4.1) that was fed to CPB was calculated based on the estimated amount of Co adsorbed during the breakthrough experiments (578 mg ±10%). According to Fig. 10, the effluent pH decreased to pH~2. A smaller slope shows the effect of the second column and higher pH in generating weak interactions of the Dowex with Li, Mn, and Al. However, saturation for these metals is achieved before Co breakthrough. The mass transfer zone is also extended for Fe, which is easily released after reaching breakthrough. Zn closely follows the Co profile, while the higher affinity and low concentrations of Ni completely remove it from the effluent (Table 3).

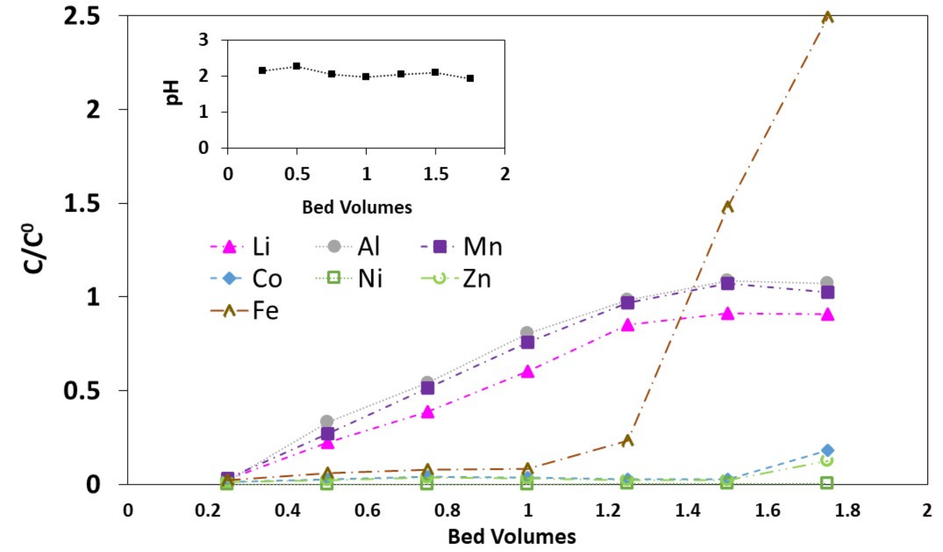

Fig. 10. Load profile for the effluent collected after the feed solution is passed through CPB. The inset graph shows the corresponding pH profile.

After loading, the lead column in CPB was washed with 40 mL of DI water. Although the second column was used to trap Co washed away from the lead column, Fig. 11 shows that ~26% of the Co was lost in the wash. Co elution was then performed by feeding 10 mL of 0.25 M H_2SO_4, followed by 20 mL of DI water directly to the second column from top to bottom. A more dilute acid than that used for the elution shown in Fig. 5 was used to maintain a pH higher than 2 in the eluate, thus avoiding the co-elution of Ni. 45% of Co reports to the eluate with an average purity of 98.9%, where Fe and Ni were the highest impurities at 0.4 and 0.3%, respectively. Cobalt concentration at the last elution point (1858 mg/L) suggests that a longer elution would have been required to completely elute the Co.

94% of the fed Ni remained within the adsorption columns, and since no acid was directly fed to the lead column, most of the Ni would be expected to stay in this column. A pH below 2 featured for the last point of the elution (Fig. 11) without appearance of Ni confirm this. The process could be repeated until the lead column is saturated with Ni and then regenerated with 2 M H_2SO_4.

The final effluent, which corresponds to the Li/Mn solution contains less than 6% of the initial Co and less than 0.1% of the initial Ni. Average concentration of the Li/Mn concentrate is shown in Table 1.

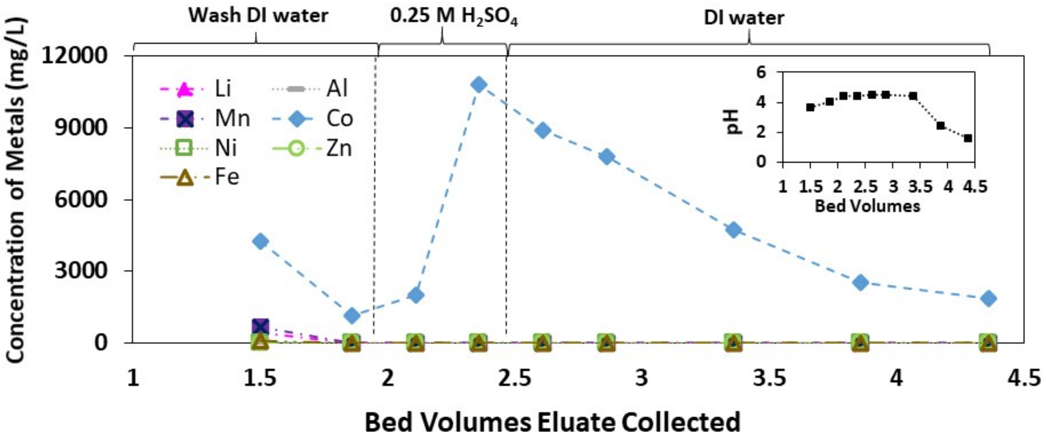

Fig. 11. Elution profile for Co concentrate eluted from CPB. The inset graph shows the corresponding information for the pH.

	Li	Al	Mn	Fe	Co	Ni	Zn
Feed (ppm)	2881.22	331.07	4310.71	526.05	17571.46	830.37	45.23
% Effluent	65.14	80.59	77.26	74.12	5.88	0.14	4.59
% Wash	14.57	21.95	15.80	24.52	25.80	2.70	29.28
% Eluate	0.02	0.05	0.02	6.11	45.29	3.02	48.14
% Not Eluted	20.27	0.00	6.92	0.00	23.03	94.13	17.98
% Total	100.00	102.59	100.00	104.75	100.00	100.00	100.00

Separation factors for the two sets of columns are listed in Tables 4 and 5. Regarding CPA, high separation factors are observed for Ni over Li, Mn, Co and Fe. For most of the elements, these values are an order of magnitude higher than those reported by Liebenberg et al. (2013), 350 for Ni/Co separation at pH=2. Better separation could be attributed to the effect of loading at lower (pH~1.1) but also to the effect of extending the mass transfer zone. Grinstead (1984) reports separation factors of Ni/Fe~6 and Ni/Co~52 at pH=2, while the values obtained here (Ni/Fe=407 and Ni/Al=67) show that the Dowex resin allows separation of Ni as well as purification from common contaminants. Moreover, the impurities are not poisoning the resin as Table 2 shows that all Fe, Al, and Zn are eluted from the system.

Table 4. Separation Factors for individual metals through CPA.

Elements	$^{Li}/_{y}$	$^{Al}/_{y}$	$^{Mn}/_{y}$	$^{Fe}/_{y}$	$^{Co}/_{y}$	$^{Ni}/_{y}$	$^{Zn}/_{y}$
$^{x}/_{\mathrm{Li}}$	1	40.80	0.45	6.70	1.26	2732.59	51.90
$^{x}/_{\mathrm{Al}}$	0.02	1	0.01	0.16	0.03	66.98	1.27
$^{x}/_{\mathrm{Mn}}$	2.25	91.66	1	15.06	2.83	6139.53	116.60
$^{x}/_{\mathrm{Fe}}$	0.15	6.09	0.07	1	0.19	407.58	7.74
$^{x}/_{\mathrm{Co}}$	0.79	32.35	0.35	5.32	1	2166.56	41.15
$^{x}/_{\mathrm{Ni}}$	0.00	0.01	0.00	0.00	0.00	1	0.02
$^{x}/_{\mathrm{Zn}}$	0.02	0.79	0.01	0.13	0.02	52.65	1

Table 5 features similar observations for CPB. High separation factors are achieved for Co over Mn and Li suggesting that the Dowex can be used effectively to isolate Co from the leachate. To our knowledge this is the first work that demonstrates an effective Co/Mn separation from a Co rich feed using Dowex. Accordingly, the separation factors reported for Co over impurities such as Al suggest easy removal from Co concentrate. Separation of Fe is lower, while Zn closely follows Co. An additional separation step would be required for complete removal of these elements. Table 3 shows that Al, Fe and almost all Zn is eluted from the system. The separation factor calculated for Co/Ni of 15 is higher than any value for IX attained from other papers but lower than the values reported for SX at room temperature (Chiu & Chen, 2017, Grinstead, 1984 , Tanaka et al., 2013,Tait, 1993).

Table 5. Separation factors of individual metals through CPB.

Elements	$^{Li}/_{y}$	$^{Al}/_{y}$	$^{Mn}/_{y}$	$^{Fe}/_{y}$	$^{Co}/_{y}$	$^{Ni}/_{y}$	$^{Zn}/_{y}$
$^{x}/_{Li}$	1	2.30	0.85	282.59	2093.23	139.66	2225.32
$^{x}/_{Al}$	0.43	1	0.37	122.67	908.65	60.63	965.99
$^{x}/_{Mn}$	1.18	2.72	1	333.45	2470.01	164.80	2625.88
$^{x}/_{Fe}$	0.00	0.01	0.00	1	7.41	0.49	7.87
$^{x}/_{Co}$	0.00	0.00	0.00	0.14	1	0.07	1.06
$^{x}/_{Ni}$	0.01	0.02	0.01	2.02	14.99	1	15.93
$^{x}/_{Zn}$	0.00	0.00	0.00	0.13	0.94	0.06	1

5.0 Concentrate Analysis

Precipitation of the Ni and Co from the eluates was performed by the addition of 2 M NaOH to achieve pH=11. XRD analysis of the precipitates (Fig. 12) confirmed the formation of $Ni(OH)_2$ and $Co(OH)_2$. The XRD of the precipitate $Ni(OH)_2$ (Fig. 12 a) displays a semi-crystalline solid which would be expected from small crystals—as determined from the Scherrer Equation. Composition of the precipitated hydroxides, in metal basis are shown in Table 6. A 99.0% purity was achieved for Ni, while to Co purity reached 98.5%.

The major metal impurity in the Ni concentrate is Co at 0.73%. Optimization of the washing process is required to achieve higher purities. The major impurity of the $Co(OH)_2$ was Fe at 0.55%. For CPB, pH control of the elution allowed keeping Ni concentration at a minimum of 0.5%, but further optimization is required.

Table 6. Concentration of the precipitated Co and Ni hydroxides.

	Co (%)	**Ni (%)**	**Fe (%)**	**Zn (%)**	**Mn (%)**	**Al (%)**	**Cu (%)**
$Co(OH)_2$	98.54	0.50	0.55	0.35	0.03	0.02	0
$Ni(OH)_2$	0.73	99.0	0.15	0	0.07	0.03	0.02

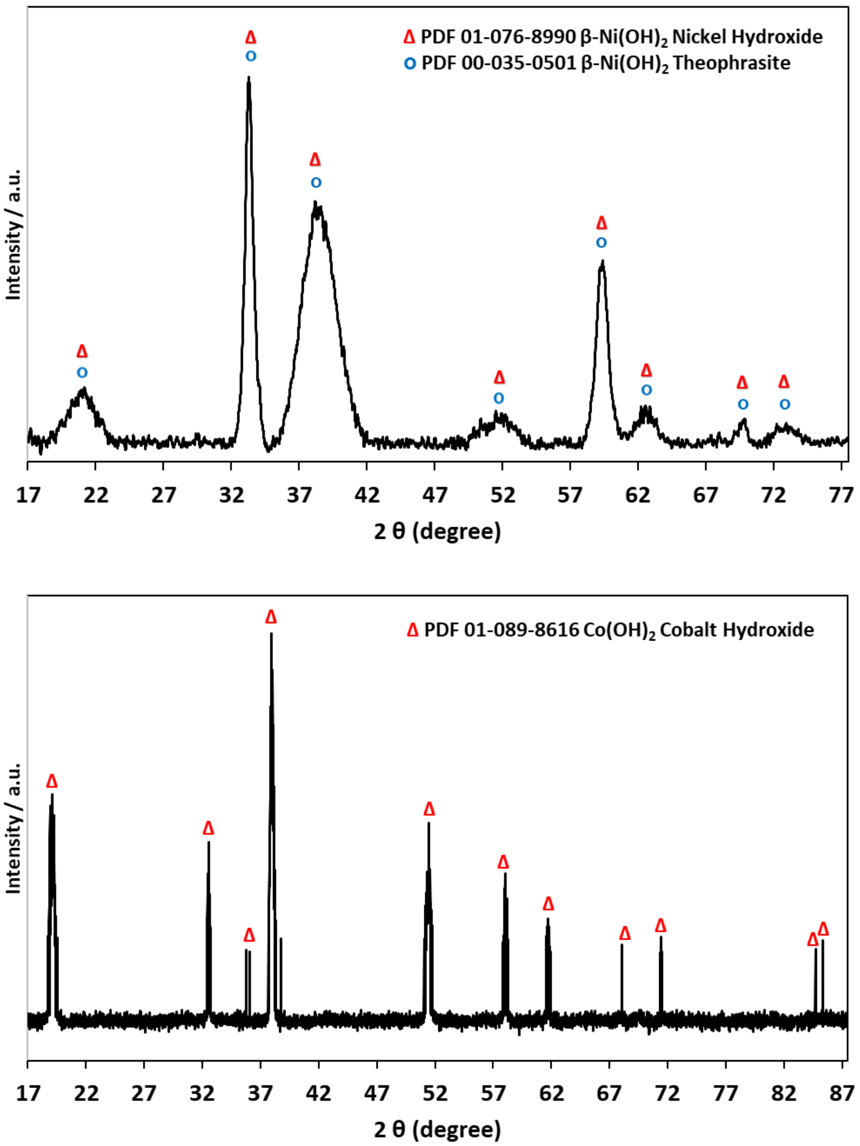

Fig. 12. XRD of Ni Concentrate & Co Concentrate precipitated after CPA & CPB elution

6. Conclusion

Dowex M4195 resin was successfully used to separate and purify Ni and Co from LIB leachates with minimum chemical consumption and pH adjustment. Using two pairs of columns that were connected in series were used to selectively 99.0% Ni and 98.5% Co products were isolated from LIB leachate solutions containing contaminants of Fe, Al, and Zn. Our observed separation factors for CPA were Ni/Co=2170 and Ni/Fe=408, Ni/Al=61, Ni/Zn=53 using a feed pH=1.1, and the separation factors for CPB were Co/Ni=15, Co/Fe=7.41, Co/Al=909, Co/Zn=0.94 with a feed pH=4.1. In addition, no pre-treatment of the leachate was necessary, due to the large separation factors between the target metals and impurities. Overall, this IX separation process represents an alternative to solvent extraction, where the processed LIB leachate solutions can effectively separate and recover Co and Ni without being affected by contaminant metals.

Appendix A. Supplementary data (Word File)

Acknowledgments

This manuscript has been authored by Battelle Energy Alliance, LLC under Contract No. DE-AC07-05ID14517 with the U.S. Department of Energy. This work was supported by the Critical Materials Institute, an Energy Innovation Hub funded by the U.S. Department of Energy, Office of Energy Efficiency and Renewable Energy, Advanced Manufacturing Office. The authors would like to acknowledge Retriev Technologies (Richard Schutte and Kathy Bruce) for providing the lithium battery scrap feed used the leachate in this study. The team is grateful for their technical assistance.

Declaration of Competing Interests

The authors declare that they have no known competing financial interests or personal relationships that could have appeared to influence the work reported in this paper.

References

Agarwal, V., Khalid, M.K., Porvali, A., Wilson, B.P. and Lundström, M., 2019. Recycling of spent NiMH batteries: Integration of battery leach solution into primary Ni production using solvent extraction. Sustainable Materials and Technologies, 22: e00121.

Armand, M. et al., 2020. Lithium-ion batteries – Current state of the art and anticipated developments. Journal of Power Sources, 479: 228708.

Atia, T.A., Elia, G., Hahn, R., Altimari, P. and Pagnanelli, F., 2019. Closed-loop hydrometallurgical treatment of end-of-life lithium ion batteries: Towards zero-waste process and metal recycling in advanced batteries. Journal of Energy Chemistry, 35: 220-227.

Campbell, G.A., 2019. The cobalt market revisited. Mineral Economics, 33(1-2): 21-28.

Chiu, K.-L. and Chen, W.-S., 2017. Recovery and Separation of Valuable Metals from Cathode Materials of Spent Lithium-Ion Batteries (LIBs) by Ion Exchange. Science of Advanced Materials, 9(12): 2155-2160.

DeRousseau, M., Gully, B., Taylor, C., Apelian, D. and Wang, Y., 2017. Repurposing Used Electric Car Batteries: A Review of Options. JOM, 69(9): 1575-1582.

Diaz, L.A. et al., 2020. Electrochemical-assisted leaching of active materials from lithium ion batteries. Resources, Conservation and Recycling, 161: 104900.

Diniz, C.V., Ciminelli, V.S.T. and Doyle, F.M., 2005. The use of the chelating resin Dowex M-4195 in the adsorption of selected heavy metal ions from manganese solutions. Hydrometallurgy, 78(3-4): 147-155.

Gates-Rector, S. and Blanton, T., 2019. The Powder Diffraction File: a quality materials characterization database. Powder Diffraction, 34(4): 352-360.

Grinstead, R.R., 1984. Selective absorption of copper, nickel, cobalt and other transition metal ions from sulfuric acid solutions with the chelating ion exchange resin XFS 4195. Hydrometallurgy, 12(3): 387-400.

Jacoby, M., 2019. It's time to get serious about recycling lithium-ion batteries, Chemical & Engineering News.

Koivula, R., Lehto, J., Pajo, L., Gale, T. and Leinonen, H., 2000. Purification of metal plating rinse waters with chelating ion exchangers. Hydrometallurgy, 56(1): 93-108.

Kurşunoglu, S., 2019. EXTRACTION OF NICKEL FROM A MIXED NICKEL-COBALT HYDROXIDE PRECIPITATE. Bilimsel Madencilik Dergisi: 45-52.

Lannoo, S., Vilas-Boas, A., Sadeghi, S.M., Jesus, J. and Soares, H.M.V.M., 2019. An environmentally friendly closed loop process to recycle raw materials from spent alkaline batteries. Journal of Cleaner Production, 236: 117612.

Larouche, F. et al., 2020. Progress and Status of Hydrometallurgical and Direct Recycling of Li-Ion Batteries and Beyond. Materials, 13(3): 801.

Lee, K.K., Yoon, W.S., Kim, K.B., Lee, K.Y. and Hong, S.T., 2001. Characterization of LiNi0.85Co0.10M0.05O2 (M = Al, Fe) as a cathode material for lithium secondary batteries.

Journal of Power Sources, 97-98: 308-312.
Liebenberg, C., Dorfling, C., Bradshaw, S., Akdogan, G. and Eksteen, J., 2013. The recovery of nickel and cobalt from a sulphate bioleach solution using Dow M4195, The Southern African Institute of Mining and Metallurgy Base Metals Conference, pp. 269-282.
Linnenkoper, K., 2019. The unknown success of lithium-ion battery recycling, Recycling International.
Manthiram, A., 2020. A reflection on lithium-ion battery cathode chemistry. Nature Communications, 11(1).
Mendes, F.D. and Martins, A.H., 2004. Selective sorption of nickel and cobalt from sulphate solutions using chelating resins. International Journal of Mineral Processing, 74(1-4): 359-371.
Mizushima, K., Jones, P., Wiseman, P. and Goodenough, J., 1981. LixCoO2 (0<x⩽1): A new cathode material for batteries of high energy density. Solid State Ionics, 3-4: 171-174.
Nagib, S., Inoue, K., Yamaguchi, T. and Tamaru, T., 1999. Recovery of Ni from a large excess of Al generated from spent hydrodesulfurization catalyst using picolylamine type chelating resin and complexane types of chemically modified chitosan. Hydrometallurgy, 51(1): 73-85.
Nayl, A.A., Hamed, M.M. and Rizk, S.E., 2015. Selective extraction and separation of metal values from leach liquor of mixed spent Li-ion batteries. Journal of the Taiwan Institute of Chemical Engineers, 55: 119-125.
Nguyen, R.T., Eggert, R.G., Severson, M.H. and Anderson, C.G., 2021. Global Electrification of Vehicles and Intertwined Material Supply Chains of Cobalt, Copper and Nickel. Resources, Conservation and Recycling, 167: 105198.
Ocio, A. and Elizalde, M.P., 2011. Iron(III) Extraction from Phosphoric Acid Solutions by Cyanex 301. Solvent Extraction and Ion Exchange, 29(3): 337-362.
Olivetti, E.A., Ceder, G., Gaustad, G.G. and Fu, X., 2017. Lithium-Ion Battery Supply Chain Considerations: Analysis of Potential Bottlenecks in Critical Metals. Joule, 1(2): 229-243.
Peng, F. et al., 2019. Impurity removal with highly selective and efficient methods and the recycling of transition metals from spent lithium-ion batteries. RSC Adv., 9(38): 21922-21930.
Pinegar, H. and Smith, Y.R., 2019. Recycling of End-of-Life Lithium Ion Batteries, Part I: Commercial Processes. Journal of Sustainable Metallurgy, 5(3): 402-416.
Pranolo, Y., Zhang, W. and Cheng, C.Y., 2010. Recovery of metals from spent lithium-ion battery leach solutions with a mixed solvent extractant system. Hydrometallurgy, 102(1-4): 37-42.
Rosato, L., Harris, G.B. and Stanley, R.W., 1984. Separation of nickel from cobalt in sulphate medium by ion exchange. Hydrometallurgy, 13(1): 33-44.
Sadanandam, R. et al., 2008. Production of high purity cobalt oxalate from spent ammonia cracker catalyst. Hydrometallurgy, 91(1): 28-34.
Sloop, S.E. et al., 2019. Cathode healing methods for recycling of lithium-ion batteries. Sustainable Materials and Technologies, 22: e00113.
Sole, K.C., Mooiman, M.B. and Hardwick, E., 2017. Ion Exchange in Hydrometallurgical Processing: An Overview and Selected Applications. Separation & Purification Reviews, 47(2): 159-178.
Swartz, B., Donegan, S. and Amos, S., 2009. Processing considerations for cobalt recovery from Congolese copperbelt ores. Hydrometallurgy: 385-400.
Virolainen, S., Wesselborg, T., Kaukinen, A. and Sainio, T., 2021. Removal of iron, aluminium, manganese and copper from leach solutions of lithium-ion battery waste using ion exchange. Hydrometallurgy, 202: 105602.
Willuhn, M., 2019. Lithium batteries – 1.2m tons ready for recycling by 2030, https://www.pv-magazine.com/.
Xu, P. et al., 2020. Efficient Direct Recycling of Lithium-Ion Battery Cathodes by Targeted Healing. Joule, 4(12): 2609-2626.
Zeng, X. et al., 2019. Commercialization of Lithium Battery Technologies for Electric Vehicles. Advanced Energy Materials, 9(27): 1900161.